MECHANICS AND OPTICS OF ROTATING PARTICLES AND DROPS IN GAS FLOWS

Z. M. Maksimov and A. L. Stasenko

UDC 533.6.011.8

The mechanics of flows of disperse gases and vapor droplets with allowance for the many processes of mass, momentum, and energy transfer between phases has been thoroughly investigated to date [1-3]. Far less attention has been given to the kind of nonequilibrium process found in the rotation of dispersed particles when they collide, e.g., in the vicinity of the critical cross section of a nozzle [4]. In the case of liquid drops, rotation leads to their deformation, changes the heat- and mass-transfer coefficients, and alters their force interaction with the gas. Vasenin et al. [4] have investigated the equilibrium shapes of rotating drops restrained by the forces of surface tension, which keeps them from breaking up, and they formulated the mechanics of a mixture containing rotating particles exposed to continuous flow.

In the present article we discuss the mechanics and heat and mass transfer of rotating drops in the following aspects. Firstly, finely dispersed particles can enter into the free molecular flow regime even inside the nozzle because of rapid expansion of the carrier gas [5], or they can enter into a distinctly rarefied (relative to particles) medium [6]. Secondly, the onset of a lateral force (of the Magnus type) will necessarily impart a transverse displacement to the particles and cause their trajectories to intermingle. Thirdly, there is a domain of parameters of the particles and the gas flowing around them where the temperature equalization time in the particle volume is commensurate with the time constants of other relaxation processes, making it necessary to solve the heat-conduction equation inside an ellipsoidal particle. Fourthly, both the self-radiation from a small (comparable with the characteristic wavelength) particle and externally incident radiation scattered by it depend on the shape of the particle [7], so that the optical characteristics of a vapor–drop flow with rotating particles can differ, in general, from what they would be in the absence of rotation.

The dynamics of a rotating sphere in free molecular flow has been investigated previously [8], but an expression was not given for the drag torque. Expressions have been derived [9] for the lift-to-drag ratios of various bodies moving in a rarefied gas "at satellite velocities," along with the additional forces and torques generated by the slow rotation of certain bodies (a circular cylinder and a cone), subject to the condition that the flow velocity around the body is much greater than the circumferential velocity associated with rotation. The rotational derivatives of rapidly moving (in the supersonic approximation) bodies with a fixed geometry have been investigated [10]. In application to the mechanics of multiphase jets it is necessary to expand the force and torque expressions for all values of the dimensionless flow velocity $S = U/\sqrt{2RT}$ and the relative circumferential velocity $|\omega \times \mathbf{r}|/U$ (particularly in the case of rotation of a spherical particle whose center of mass is fixed relative to a surrounding element of the carrier medium).

Of all the possible relative positions of the flow velocity vector and the particle angular momentum vector, we choose the orthogonal case ($\omega \perp U$), which has direct bearing on the mechanics of two-phase jets: it has been noted in studies of two-phase nozzle flows [4] that the angular velocities of the particles are mainly perpendicular to the flow axis because of their collision in the vicinity of the critical cross section.

1. STATEMENT OF THE PROBLEM

We consider a drop that rotates with an angular velocity and is immersed in a free molecular flow of a carrier gas with a relative velocity $\mathbf{U} = \mathbf{V} - \mathbf{V}_p$. The main assumptions are as follows: 1) investigations of the equilibrium of a drop have shown [4] that it has an oblate ellipsoidal shape under the condition $\alpha^* = \rho^0 a_p^3 \omega^2/\sigma^0 \lesssim 2.5$ (σ^0, ρ^0 are the coefficient of surface tension and the density of the liquid, and a_p is the radius of a volume-

Moscow. Translated from Zhurnal Prikladnoi Mekhaniki i Tekhnicheskoi Fiziki, No. 5, pp. 103-110, September-October, 1989. Original article submitted May 31, 1988.

 0021-8944/89/3005-0770$12.50

equivalent sphere); 2) it is evident from experimental work that in order for a nonrotating drop to preserve its shape in an impingent flow, the dimensionless Weber number $We = 2a_p \rho U^2/\sigma^0$ (ρ is the density of the gas) must not exceed the critical value $We^* = 10$; consequently, We must be much smaller than We^* in order for the oblateness of the drop in the impingent flow to be disregarded. This requirement can be rewritten as a constraint on the dimensionless flow velocity $S^2 \ll 3p_L/p$ ($p_L = 2\sigma^0/a_p$ is the Laplacian pressure in the interior of a spherical drop, and $p = \rho RT$ is the static pressure in the gas flow); 3) we also assume that the kinetic energy of the colliding molecules is not greater than the binding energy of surface molecules of the drop; otherwise collision would knock the molecules out of the drop, and this process is not described in the present article. Accordingly, $S^2 \ll L/RT$ (L is the specific heat of vaporization).

4) We estimate the influence of particle rotation on the process of heat conduction in its interior volume. Numerical calculations [11] have shown that in the case of a nonrotating spherical particle of finite thermal conductivity in a free molecular flow the temperatures of the fore and aft points of the sphere can differ appreciably (by an amount of the same order as the temperature itself) due to the strong surface inhomogeneity of the heat flux density. The time scale of temperature equalization in the sphere is well known: $\tau_W = \rho^0 c^0 a_p{}^2/\lambda^0$ (c^0, λ^0 are the specific heat and thermal conductivity of the particle material). Consequently, if the time for the particle to rotate about its axis is much smaller than this time scale ($\omega\tau_W \gg 1$), rotation makes the heat transmission in the drop independent of the azimuth angle. In this case the dissipation of energy by drag-induced friction inside the drop and the convection induced by buoyancy in the field of centrifugal forces are negligible; 5) it can be shown that the radius of the drop must be greater than 10^{-10} m in order for the ratio of the specific energy of rotational motion $\omega^2 a_p^2/2$ and the specific energy of phase transition L to be much smaller than unity. Consequently, this condition clearly holds in all cases of practical interest for the mechanics of two-phase flows: we find that the rotating particle breaks up long before its rotation begins to have any significant influence on the evaporation rate; this fact justifies our disregard of centrifugal kinetic energy in comparison with the thermal and phase-transition energies. Under this assumption, sublimating solid spherical particles remain spherical at all times.

2. SYSTEM OF EQUATIONS FOR THE MECHANICS, HEAT TRANSFER, AND MASS TRANSFER OF AN ELLIPSOIDAL DROP

An element of surface of the ellipsoid can be written in the form

$$d\Sigma^e = \frac{a^2 \sin\alpha\, d\alpha\, d\varphi}{4\pi\varepsilon^2 (1 + k^2 \sin^2\alpha)^2}, \quad \operatorname{tg}\alpha = \varepsilon^2 \operatorname{tg}\theta, \quad \varepsilon = \frac{b}{a}, \quad k^2 = \varepsilon^{-2} - 1,$$

where a and b are the semimajor and semiminor axes of the meridian cross section and θ and φ are the polar and azimuth angle in spherical coordinates.

Integration of the known mass, momentum, and energy flow densities over the surface of the rotating ellipsoid [12] yields quadratures that cannot, in general, be expressed in elementary functions:

$$\frac{dm_p}{\beta^* dt} = a^2 \left\{ \frac{\alpha_k \rho \langle c\rangle}{\sqrt{1+k^2}} \left[(1+2S^2) I_1 + 2k^2 S^2 I_2 + \sqrt{1+k^2} \exp(-S^2) \right] - \alpha_k \rho_s (T_p) \langle c(T_p)\rangle 2\Sigma^e \right\},$$

$$m_p \frac{c^0}{R} \frac{dT_p}{\beta^* dt} = a^2 \frac{2\rho\langle c\rangle}{\sqrt{1+k^2}} \left\{ \alpha_e (1-\alpha_k) \left[\frac{c_V^i}{R} (T - T_p) - 2T_p \right] + \alpha_k \frac{c_V^i}{R} T \right\} \times$$

$$\times \left[(1+2S^2) I_1 + 2k^2 S^2 I_2 + \sqrt{1+k^2} \exp(-S^2) \right] + \langle c\rangle \rho a^2 T \left[\alpha_e (1-\alpha_k) + \alpha_k \right] \left[2(1 + 3S^2 + S^4) I_1 + \right.$$

$$\left. + \left[2S^2 (2+S^2)(1+k^2) - S^2 (2S^2 + 5) \right] I_2 + (2+S^2) \sqrt{1+k^2} \exp(-S^2) \right] -$$

$$- \alpha_k \rho_s (T_p) \langle c(T_p)\rangle T_p 2 \left(2 + \frac{c_V^i}{R} \right) \Sigma^e + \frac{dm_p}{\beta^* dt} \left(L - \frac{\varkappa}{\varkappa - 1} T_p \right),$$

$$m_p \frac{d\mathbf{V}_p}{\beta^* dt} = \rho U \mathbf{U} \frac{8a^2}{\sqrt{\pi} S} \left\{ \left[(2 - \alpha_n)(1 - \alpha_k) + \alpha_k \right] \times \right.$$

$$\times \left[\frac{\sqrt{\pi}\operatorname{erf} S}{12S} \frac{3k^4 + 2S^2 (3 + (1+k^2)^2)}{k^4 \sqrt{1+k^2}} + \frac{3k^2 (1+k^2) - 8S^2}{6k^4 \sqrt{1+k^2}} I_1 - \right.$$

$$\left. \left. - \frac{5 + 3k^2}{3k^2 \sqrt{1+k^2}} S^2 I_2 - \frac{S^2}{3\sqrt{1+k^2}} I_3 - \frac{\exp(-S^2)}{2k^2} \right] + \right.$$

$$+[\alpha_k+\alpha_\tau(1-\alpha_n)]\left[\sqrt{\pi}\,S\,\mathrm{erf}\,S\,\frac{k^2-2}{3k^4}+\frac{-3k^2+8S^2}{6k^4\sqrt{1+k^2}}I_1+\right.$$
$$+\frac{k^2+S^2(10-6k^2-6k^4)}{6k^2\sqrt{1+k^2}}I_2+\frac{S}{3\sqrt{1+k^2}}I_3+\frac{1+k^2}{2k^3}\exp(-S^2)\Big]+$$
$$+\frac{\alpha_n(1-\alpha_k)}{16k^2}\sqrt{\pi\frac{T_p}{T}}\left[(1+2k^2)(2\Sigma^e-1)-1\right]\Big\}+$$
$$+\frac{4}{3}[\alpha_\tau(1-\alpha_k)+\alpha_k](\boldsymbol{\omega}\times\mathbf{U}),$$

$$\frac{J^e\,d\boldsymbol{\omega}}{\beta^*\,dt}=-\frac{5}{4}\frac{\rho a^4U\boldsymbol{\omega}}{\sqrt{\pi}\,S}[\alpha_\tau(1-\alpha_k)+\alpha_k]\left\{\frac{8k^4+3k^3+1-2S^2(1+k^2)^2}{k^4\sqrt{1+k^2}}I_1+\right.$$
$$+\frac{2S^2[4k^4+k^2+1-2(1+k^2)(k^2-S^2)]-4k^4+k^2}{k^4}\sqrt{1+k^2}\,I_2+$$
$$\left.+\frac{2k^4-2k^2+2(1+k^2)S^2-1}{k^4}\exp(-S^2)\right\},$$

$$m_p=a_p^3=a^2b=\varepsilon a^3,\quad J^e=\varepsilon a^5,\quad \beta^*=\frac{3}{8}\frac{\rho^*}{\rho^0}\frac{r^*}{a_p^*},$$

$$I_n=\int_0^1\frac{x^{2(n-1)}\exp(-S^2x^2)}{(1+k^2x^2)^{1/2}}\,dx,$$

$$\Sigma^e=a^2\left(\frac{1}{2}+\frac{1}{4k\sqrt{1+k^2}}\ln\frac{\sqrt{1+k^2}+k}{\sqrt{1+k^2}-k}\right).$$

Here m_p, J^e, and Σ^e are the mass, moment of inertia about the rotation axis, and the surface area of the ellipsoid, $c_V{}^i$ is the specific heat of molecular internal degrees of freedom, α_k, α_e, α_n, and α_τ are the energy coefficients of condensation and accommodation and the normal and tangential components of the momentum (these coefficients are taken equal to unity in the ensuing calculations). We assume that equilibrium exists in all degrees of freedom.

The system of equations is closed by the algebraic function $\varepsilon(\alpha^*)$, whose exact expression is given in [4] and which can be represented approximately by a straight line $\varepsilon \approx 1 + \alpha^*/8$ (in the interval $\alpha^* < 2.5$ corresponding to an ellipsoid of revolution). In this system of equations the values of the gasdynamic parameters are normalized to the appropriate scales of density ρ^*, velocity V^*, temperature T^*, and distance r^*; the time scale is $t^* = r^*/V^*$, and the particle radii a and b are normalized to the radius a_p^* of the volume-equivalent sphere. In the calculations we set these scales equal to the values of the parameters in the initial cross section $x = 0$.

Radiation energy losses are disregarded in the equations describing the heat content of the particle. This assumption is particularly justified insofar as a small particle does not radiate the entire spectrum of the solid body, but only the spectrum cut off at the long-wavelength end [13]. The input temperature T_p in this system corresponds to the hypothesis of a volumetrically isothermal particle.

In addition to the given system, we solve the equation for heat conduction in the particle interior

$$\rho^0c^0\frac{\partial T^0}{\partial t}=\frac{1}{r}\frac{\partial}{\partial r}\left(\lambda^0 r\frac{\partial T^0}{\partial r}\right)+\frac{\partial^2(\lambda^0T^0)}{\partial z^2}$$

subject to the boundary condition $\partial T^0/\partial N|_\Gamma = \gamma^* q$, where the surface energy flux density normalized to $\rho^* a^{*3}$ has the form

$$q=\frac{1}{8}\rho T^{3/2}\sqrt{\frac{2}{\pi\varkappa}}\left\{Q_1\left[S^2+\frac{7\varkappa-5}{2(\varkappa-1)}\right]+Q_2 2S^2\left(S^2+\frac{2\varkappa-1}{\varkappa-1}\right)\right\}-$$
$$-\frac{3\varkappa-1}{8(\varkappa-1)}p_s(T_\Gamma^0)\sqrt{\frac{8}{\pi}T_\Gamma^0},$$

$$Q_j=\int_0^{\pi/2}\exp(-S^2\cos^2\theta\sin^2\alpha)(\sin\theta\sin\alpha)^{2(j-1)}\,d\theta,\quad j=1,2;$$

$$\gamma^*=\rho^*a^{*3}a_p^*(T^*\lambda^0)^{-1},\quad a^*\equiv V^*;$$

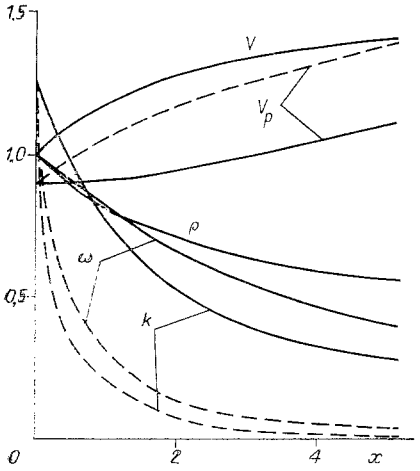

Fig. 1

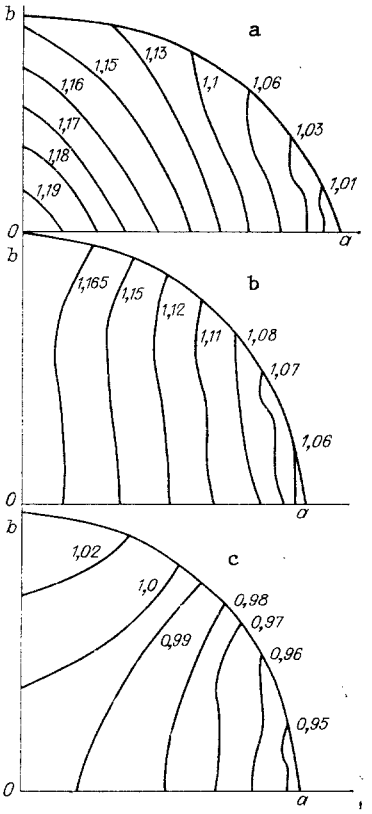

Fig. 2

the saturation pressure p_s in the liquid–vapor phase transition is normalized to $\rho^* a^{*2}$. (Here, for simplicity, all the accommodation coefficients have already been set equal to unity.)

3. RESULTS OF A NUMERICAL ANALYSIS OF THE DYNAMICS, HEAT TRANSFER, AND MASS TRANSFER OF A ROTATING PARTICLE

The well-known three-layer Dufort–Frankel scheme [14], which is stable for any relations between the time step τ and the spatial step h within error limits of the order $\Pi = O(\tau^2 + h^2 + (\tau/h)^2)$, is used for the integration of the heat-conduction equation in the interior of the particle. For $\tau = h^2$ and $h < 10^{-1}$ we have $\Pi < 10^{-2}$. We give the results of a numerical analysis of the dynamics and heat and mass transfer of particles accelerated by a quasi-one-dimensional flow, whose cross section varies linearly along the axial coordinate: $F/F^* = 1 + x/20$. We investigate solid spherical particles and deformed liquid drops, whose angular velocity is limited by their ellipsoidal configuration (here $\alpha^* = 2.5$). The thermophysical properties of the substances (density, surface tension, specific heat, thermal conductivity, heat of phase transition, and saturated vapor pressure) are approximated by simple functions of the temperature on the basis of tabulated data. The values of the dimensionless parameters of the problem κ, α^*, β^*, γ^*, L, c^0/R are given below.

Figure 1 shows the downstream distributions of the velocity, density of the gas, and the parameters of a rotating liquid metal oxide particle of constant mass for two sets of dimensionless parameters corresponding to a five-fold difference only in the value of the characteristic density of the gas. Clearly, as the density increases, the angular velocity and eccentricity of the particle decreases more and more rapidly, and the linear velocity quickly relaxes to the velocity of the gas. Here $\kappa = 1.4$, $R/c^0 = 0.21$, the solid curves correspond to $\beta^* = 4.7 \times 10^{-2}$ and $\gamma^* = 0.31$, and the dashed curves correspond to values of 0.235 and 1.55 for these quantities.

Figure 2 shows the shape of the surface and isotherms in the volume of the particle at three successive times. (We recall that the temperature scale is the initial value of the gas temperature T^*.) We see that only regions of the rotating drop close to its equator experience any cooling at the first of these times [$t_1 = 0.05$, $x_1 = 0.418$ (a)], whereas its central regions are still surrounded by closed equal-temperature surfaces with values ap-

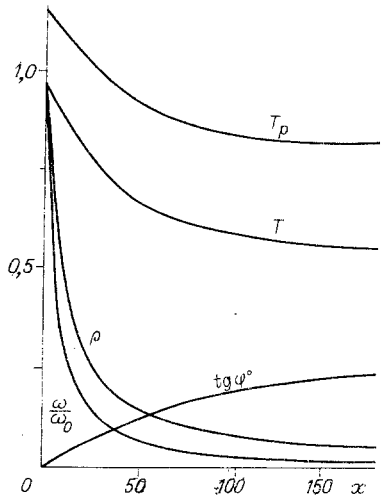

Fig. 3

proximately equal to the temperature specified at the initial time $T_p^* = 1.2$. Subsequently, [at time $t_2 = 0.1$, $x_2 = 0.92$ (b)] the isothermal surfaces become almost cylindrical, and with further slowing of rotation [$t_3 = 0.5$, $x_3 = 6.25$ (c)] the drop is almost spherical and volumetrically isothermal. The values of the coordinate indicated for these times can be used to "tie in" the isothermal patterns with the parameters of the particle and the gas in Fig. 1 (dashed curves).

Figure 3 shows the variation of the deviation (perpendicular to the axis) of the trajectory of a rotating solid spherical particle; we see that the angular deviation $\varphi^0 = \tan^{-1}(y/x)$ attains 10° in this example. As a result, the number of particle collisions in the multiphase flow can increase. The initial value of the angular velocity of the particle is chosen so as to achieve a uniform energy distribution among the degrees of freedom in application to particle chaos (where the energies of rotational and translational motion are of the same order) and is two orders of magnitude greater than the limiting angular velocity in the case of a liquid particle of the same material. The same figure illustrates the strong thermal nonequilibrium of the particle and the carrier gas. Here $\kappa = 1.4$, $\beta^* = 0.235$, $\gamma^* = 1.55$, and $\omega_0 = 10^3$.

Figure 4 shows the analogous parameters for a drop accelerated by vapor of the same substance and subjected to surface phase transitions. The capricious variation of the mass and

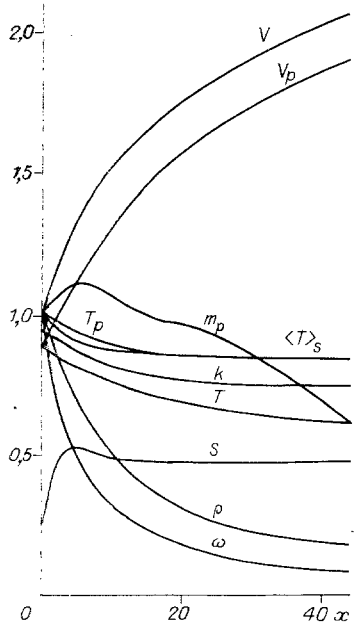

Fig. 4

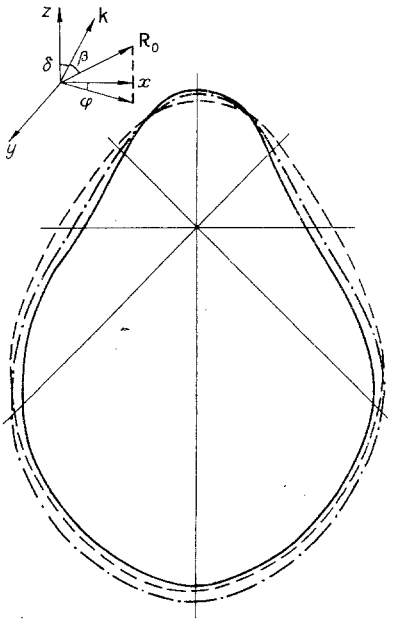

Fig. 5

slip along the coordinate is attributable to the fact that vapor is injected into the flow at the initial point of the drop in such a way as to establish conditions for condensation on its surface. As a result, its mass increases at first and then decreases monotonically due to the prevalence of evaporation. In this case the mean surface temperature $\langle T\rangle_s$ is lower than the isothermal temperature T_p at the initial times, but then they eventually equalize. The slip and temperature of the drop rapidly approach almost constant values (within the limits of the figure), and the eccentricity remains constant as well, despite the appreciable monotonic decrease in the angular velocity, indicating much stronger evaporation at the poles than at the equator (the temperature is higher at the poles; cf. Fig. 2). Here $\kappa = 9/8$, $\beta^* = 0.26$, $\gamma^* = 1.12$, $R/c^0 = 0.058$, $L = 13.83$, $p_s = 4.1 \times 10^{-3} \exp(20.295 - 13.4/T)$.

4. OPTICS OF AN ELLIPSOIDAL PARTICLE: SCATTERING OF EXTERNAL RADIATION

The scattering of an electromagnetic wave by an ellipsoid of material having a specific complex refractive index $m = n_1 - in_2$ is analyzed on the basis of a method, which is analogous to Mie theory for a sphere and is described, e.g., in [7], for solving the Maxwell equations outside and inside the investigated body. Taking into account the smallness of the deformation of a drop in comparison with a sphere and restricting the expansions to the first terms, we obtain expressions for the components of the electric field diffracted by the ellipsoid:

$$E_\varphi = -\frac{iE_0}{kr}\sin\varphi\exp(-ikr)\left\{\sum_{l=1}^{\infty}(c_lQ_l + b_lS_l) + i\frac{m^2-1}{4\pi m^2}k^3V^eF(\delta,\beta)\right\},$$

$$E_\beta = -\frac{iE_0}{kr}\cos\varphi\exp(-ikr)\left\{\sum_{l=1}^{\infty}(c_lS_l + b_lQ_l) - i\frac{m^2-1}{4\pi m^2}k^3V^eF(\delta,\beta)\cos\varphi\right\},$$

where $Q_l = P_l^1(\cos\beta)/\sin\beta$; $S_l = -P_l^1(\cos\beta)\sin\beta$; P_l^1 are first-order Legendre polynomials, $V^e = (4/3)\pi a^2 b = (4/3)\pi a_p^3$ is the volume of the ellipsoid or an equivalent sphere of radius a_p; $k = 2\pi/\lambda$ is the wave number, δ is the angle between the incident wave vector $\mathbf{k}$ and the z axis, β is the angle between the vector $\mathbf{k}$ and the direction of observation $\mathbf{R}_0$; and φ is the azimuth angle of the direction $\mathbf{R}_0$ in polar coordinates ($-\mathbf{k}$, $\mathbf{E}$, $\mathbf{H}$) (Fig. 5).

The coefficients of the expansion in Legendre polynomials are well-known:

$$c_l = \frac{2l+1}{l(l+1)}\frac{\psi_l(\zeta)\psi_l'(m\zeta) - m\psi_l'(\zeta)\psi_l(m\zeta)}{\xi_l(\zeta)\psi_l(m\zeta) - m\xi_l'(\zeta)\psi_l(m\zeta)},$$

$$b_l = \frac{2l+1}{l(l+1)}\frac{\psi_l'(\zeta)\psi_l(m\zeta) - m\psi_l(\zeta)\psi_l'(m\zeta)}{\xi_l(\zeta)\psi_l(m\zeta) - m\psi_l'(m\zeta)\xi_l(\zeta)}.$$

Here

$$\psi_l(\zeta) = \sqrt{\frac{\pi\zeta}{2}}J_{l+1/2}(\zeta);\quad \xi_l(\zeta) = \sqrt{\frac{\pi\zeta}{2}}H^{(2)}_{l+1/2}(\zeta);\qquad \zeta = 2\pi a_p/\lambda;$$

$J_{l+1/2}$, $H_{l+1/2}^{(2)}$ are Bessel functions and Hankel functions of the second kind of half-integer orders.

We note that the corrections for the ellipsoidal geometry in the expressions for E_φ and E_β are more precise than in the expansions of the functions only in the small quantities $(m^2 - 1)/4\pi m^2$ [7]. This means considerable relaxation of the demand for smallness of the deviation of the modulus of the refractive index from unity. For example, the error is of the order of 5% for $b/a = \varepsilon = 0.5$ and $m = 2$.

Figure 5 shows the angular scattering diagrams for a monochromatic unpolarized plane electromagnetic wave incident on a sphere (solid curve) and on an ellipsoidal particle for two directions of incidence: parallel to the equatorial plane and the symmetry axis (dashed curve; the diagrams for these two cases coincide within the limits of the thickness of the dashed curve) and at the angle $\pi/4$ relative to the axis (dot-dash curve), $\zeta = 1$, $b/a = 0.835$. (We recall that the vector $\mathbf{k}$ indicates the direction of the incident wave.)

The authors are grateful to M. N. Kogan for attention and interest.

LITERATURE CITED

1. G. A. Saltanov, Nonequilibrium and Unsteady Processes in the Gas Dynamics of Single-Phase and Multiphase Media [in Russian], Nauka, Moscow (1979).

2. N. N. Yanenko, R. I. Soloukhin, A. N. Papyrin, and V. M. Fomin, Supersonic Two-Phase Flows with a Nonequilibrium Particle Velocity [in Russian], Nauka, Novosibirsk (1980).
3. S. A. Senkovenko and A. L. Stasenko, Relaxation Processes in Supersonic Gas Jets [in Russian], Énergoatomizdat, Moscow (1985).
4. I. M. Vasenin, V. A. Arkhipov, V. G. Butov, et al., Gas Dynamics of Two-Phase Nozzle Flows [in Russian], Izd. Tomsk. Gos. Univ., Tomsk (1986).
5. V. I. Blagosklonov and A. L. Stasenko, "Two-dimensional supersonic flows of a mixture of vapor and droplets in a nozzle and in a submerged jet," Izv. Akad. Nauk SSSR Énerg. Transport, No. 1 (1978).
6. V. I. Garkusha, V. M. Kuznetsov, G. V. Naberezhnova, and A. L. Stasenko, "Mixing of evaporating finely dispersed particles with an entraining gas flow," Zh. Prikl. Mekh. Tekh. Fiz., No. 3 (1982).
7. C. F. Boren and B. R. Huffman, Absorption and Scattering of Light by Small Particles, Wiley, New York (1983).
8. C.-T. Wang, "Free molecular flow over a rotating sphere," AIAA J., 10, No. 5, 713 (1972).
9. V. M. Kovtunenko, V. F. Kameko, and É. F. Yaskevich, Aerodynamics of Orbiting Spacecraft [in Russian], Naukova Dumka, Kiev (1977).
10. V. S. Galkin and L. L. Zvorykin, "Rotational derivatives of bodies in a hypersonic rarefied gas flow," Tr. Tsentr. Aérogidrodin. Inst., No. 2220 (1984).
11. V. I. Garkusha and A. L. Stasenko, "Volumetric nonisothermicity of particles in multiphase flows," Izv. Akad. Nauk SSSR, Énerg. Transport, No. 2 (1977).
12. M. N. Kogan, Rarefied Gas Dynamics [in Russian], Nauka, Moscow (1967).
13. Yu. I. Petrov, Physics of Small Particles [in Russian], Nauka, Moscow (1982).
14. A. A. Samarskii, Theory of Difference Schemes [in Russian], Nauka, Moscow (1977).

THERMAL CHARACTERISTICS OF A COUNTER-CURRENT WALL JET

V. P. Lebedev and M. I. Nizovtsev

UDC 532.526.4

Counter-current flows are widely encountered in nature and take place in different production processes and equipment. For example, counter-flowing wall jets are used in welding in an inert gas, in the gasdynamic regulation of the nozzle of a turbojet engine, and in modeling atmospheric processes. The use of gas screens [1] may be very effective in protecting elements of power-plant equipment from high-temperature gas flows. In certain cases, due to the design features of the processing equipment, thermal protection of the wall can be provided by feeding a coolant gas through a slit counter to the flow or at a large angle to the direction of its motion [2, 3]. Despite the frequent use of countercurrent wall jets in different types of equipment, their study has been limited.

Here, we experimentally investigate the process of thermal mixing of a counter-current wall jet with a gas flow, and we determine the efficiency of the thermal protection of an adiabatic wall in the direction of motion of the jet. It is shown that under certain conditions, a counter-flowing wall jet can effectively protect the wall of a channel.

A diagram of the flow we studied is shown in Fig. 1. In the tests, the counter-current wall jet was created by injecting air through a tangential slit of height s = 4.7 mm. The slit was made in the bottom wall of an aerodynamic channel with a cross section of 150 × 145 mm and a length of 1200 mm. The working wall of the channel was adiabatic and was made of glass-textolite. The velocity of the main air flow in the tests was kept at a constant value U_0 = 16 m/sec. The velocity of the secondary flow was varied from 6 to 51 m/sec. Here, the injection parameter $m = \rho_s U_s / \rho_0 U_0$ was varied within the range 0.3-2.6. The temperature of the main flow T_0 = 15-20°C, while the temperature of the secondary flow T_s = 70-80°C.

Novosibirsk. Translated from Zhurnal Prikladnoi Mekhaniki i Tekhnicheskoi Fiziki, No. 5, pp. 110-113, September-October, 1989. Original article submitted May 10, 1988.

 0021-8944/89/3005-0776$12.50